

## Spatial heterogeneity of reflected radiance from globally distributed clouds

Iliana Genkova

Pacific Northwest National Laboratory, Richland, Washington, USA

Roger Davies

Jet Propulsion Laboratory/California Institute of Technology, Pasadena, California, USA

Received 17 July 2003; revised 26 August 2003; accepted 7 October 2003; published 6 November 2003.

[1] Reflected spectral radiance measured by the Multi-angle Imaging SpectroRadiometer (MISR) on the Terra satellite has been analyzed to determine the fraction of global cloudiness that appears to be spatially homogeneous over regions of various sizes. We exclude scenes with reflectivities less than 0.2 and high latitudes to avoid snow and ice. About  $1.4 \pm 0.3\%$ , or 1 in 70, of 8.8 km cloudy regions measured at 275 m have a range of reflectivities less than  $\pm 5\%$  of the central reflectivity value of the region. This pass rate changes slightly with viewing angle, and is sensitive to the size of the test window, rising to 11% for 1.1 km regions. The pass rate rises to a value of  $2.3 \pm 0.5\%$  for 8.8 km regions if the measurement resolution is degraded to 1100 m. For the purposes of this study “global” cloudiness is limited to mid-morning clouds.

*INDEX TERMS:* 1640 Global Change: Remote sensing; 3360 Meteorology and Atmospheric Dynamics: Remote sensing; 3359 Meteorology and Atmospheric Dynamics: Radiative processes.  
**Citation:** Genkova, I., and R. Davies, Spatial heterogeneity of reflected radiance from globally distributed clouds, *Geophys. Res. Lett.*, 30(21), 2096, doi:10.1029/2003GL018194, 2003.

### 1. Introduction

[2] The optimal spatial resolution required to retrieve cloud properties on a global basis using passive remote sensing from Earth-orbiting satellites remains an open question, despite several encouraging studies [Wielicki and Parker, 1992; Di Girolamo and Davies, 1997; Oreopoulos and Davies, 1998; Rossow et al., 2002]. If the clouds can be locally shown to be approximately homogeneous, plane-parallel objects, then the conventional application of one-dimensional radiative transfer theory holds a considerable promise for the retrieval of cloud properties such as optical thickness, effective radius, and single-scatter albedo. Studies using Earth Radiation Budget Experiment (ERBE) data at 40-km resolution [Davies, 1994; Loeb and Davies, 1996], and Advanced Very High Resolution Radiometer (AVHRR) data at 4-km resolution [Loeb and Coakley, 1998], show that the plane-parallel assumption does not, however, result in consistently useful retrievals, especially when applied to nadir measurements at the investigated resolutions. For coarse-resolution satellite measurements, some of the problem may be attributed to the subpixel variability of cloud reflectivity, since the dependence of cloud reflectivity on

cloud optical depth is significantly non-linear. Other factors complicating the application of one-dimensional models are the effects of cloud side illumination, horizontal photon transport, and cloud-top structure [Loeb et al., 1997].

[3] The ERBE and AVHRR studies clearly showed that cloud heterogeneity might be a significant problem when attempting a one-dimensional retrieval of a cloud property such as optical depth. What is less clear, however, is how to quantify the frequency and degree of cloud heterogeneity on a global scale, in order to understand the errors introduced by the non-critical applications of one-dimensional radiative transfer theory.

[4] In this paper, we describe a simple quantitative measure of cloud heterogeneity obtained using globally distributed data recently acquired by the Multi-angle Imaging SpectroRadiometer (MISR) instrument on the Terra satellite at the relatively high spatial resolution of 275 m. Our intent is to examine the spatial variability of clouds on scales on the order of 1 km on a global basis and to test the assumption of local spatial invariance necessary for the application of one-dimensional theory.

[5] In the following we describe the data set used, define a convenient measure of spatial heterogeneity, and examine the general tendency of clouds to be spatially homogeneous or heterogeneous on a global scale. We note at the outset that, due to the sun-synchronous orbit of the Terra satellite, our dataset is restricted to local solar times ranging from about 10:30 to 11:00 am, irrespective of season or location. Due to the absence of afternoon cloudiness over land, in particular, the results presented here cannot be extrapolated to statements concerning global average conditions in general.

## 2. Data and Methodological Approach

### 2.1. Data Characteristics

[6] MISR [Diner et al., 1998] is a pushbroom scanner on the Terra satellite, measuring reflected solar radiance in four spectral bands with nine fixed cameras. These cameras are labeled Df, Cf, Bf, Af, An, Aa, Ba, Ca, and Da, from the most oblique forward viewing direction, through nadir to the most oblique aft viewing direction at nominal viewing angles of  $70.5^\circ$ ,  $60^\circ$ ,  $45.6^\circ$ ,  $26.1^\circ$ , and  $0^\circ$  (symmetric fore and aft). For this study only the red band (672 nm) data were used, and much of the analysis applies specifically to the An camera (i.e., nadir) data. The spatial resolution for the An camera is 250 m across-track, with a contiguous swath width of 376 km. For the remaining cameras, the

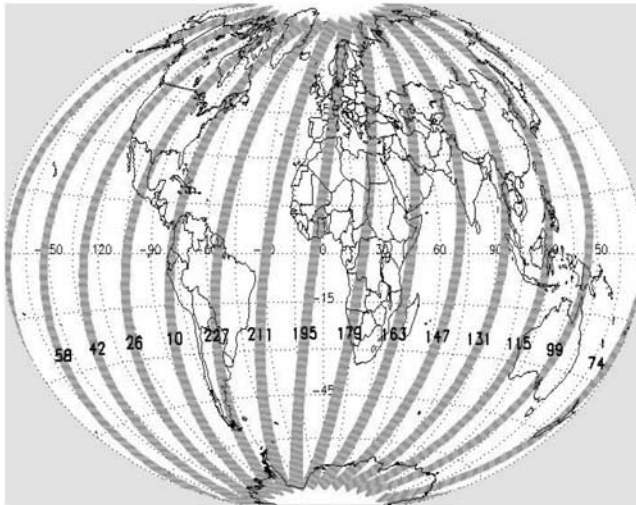


**Figure 1.** Terra's orbital paths on 9 April 2001.

across-track resolution is 275 m, with a contiguous swath width of 413 km. The along-track resolution is 214 m at nadir, rising to 750 m for the most oblique cameras, with each camera sampled every 275 m along the daylight portion of each orbit. These data are then regridded onto a uniform 275 m grid, using bi-linear interpolation. The data used in this study was the so called level 1b2 product provided by the NASA Langley Research Center. The absolute radiometric accuracy of MISR data is within (4%, with pixel-to-pixel relative accuracy (of major relevance to this study) better than 0.5% [Bruegge *et al.*, 2002].

[7] The Terra orbit is sun-synchronous, with an equator-crossing time of about 10:45 am. There are 233 distinct orbital paths covering almost the entire globe (there are no MISR data poleward of  $\sim 83^\circ$ ) and repeated once every 16 days. Routine data acquisition by MISR commenced on 24 February 2000 and has continued without significant interruption (i.e., to June 2003 at the time of writing).

[8] The basic study presented here uses data from 58 orbits, distributed over four days, one from each season (20 October 2000, 13 January 2001, 9 April 2001 and 13 July 2001). As illustrated in Figure 1, which shows the orbital paths for 9 April 2001, these orbits tend to be equally spaced around the Earth.

[9] Subsets of these data were also used for related studies. All 14 orbits from 9 April 2001 were used to estimate the effect of region size. Four of these (paths 026, 131, 211, and 227) with land/ocean coverage similar to the global average were examined in detail to study the effects of viewing angle and choice of contrast threshold.

[10] In addition, all 58 orbits were used to examine the effect of presence of ice and snow, and to suggest a procedure that would exclude snow and ice scenes at high latitudes.

## 2.2. Homogeneity Criterion

[11] A sufficient condition for a cloud to be classified as horizontally homogeneous is for the horizontal gradients within the cloud to be negligible. Given uniform boundary conditions, the cloud reflectance must then be horizontally invariant and any spatial variation in reflectance must be

directly attributable to some measure of cloud heterogeneity. For the scales of interest here, solar illumination of the cloud top is uniform, but horizontally heterogeneous land or ocean surfaces could potentially cause even a homogeneous cloud to appear heterogeneous if the cloud were thin enough. Consequently, we apply a lower threshold reflectance of 0.2 to exclude thin clouds over dark surfaces (notably ocean).

[12] This criterion will not completely exclude land surfaces from the analysis. Examination of clear land homogeneity, however, indicated that at spatial resolutions of order 1 km, the vast majority of snow-free land surfaces have spatially heterogeneous, rather than homogeneous, nadir reflectivities. Consequently there will be a slight bias in our results in favor of heterogeneity due to the presence of thin clouds over land in situations where the net reflectivity was greater than 0.2.

[13] Ocean surfaces, on the other hand, generally have a very homogeneous reflectance that is also quite low, and generally do not contribute to this bias. Exceptions occur primarily when sea-ice is present, and to a minor degree in sun-glint regions. We account for the former by limiting the latitude range of the study to the generally ice-free ocean between  $55^\circ\text{S}$  and  $65^\circ\text{N}$ . Sun glint occupies such a small percentage of our data that it was not critical to our results, and therefore received no special treatment.

[14] Horizontal variation of reflected radiances with a reflectivity,  $r > 0.2$  for low-mid latitudes is thus taken to be an approximate indicator of the presence of heterogeneous cloud. To quantify this, we first set an arbitrary threshold in the allowable spatial difference of local reflectances. If the observed differences remain below this threshold for a given region, then that region is declared horizontally homogeneous. Such a definition leads to results that depend substantially on the chosen threshold and on the area of the region, but as will be seen below, nonetheless provides a convenient shorthand description that summarizes the horizontal homogeneity of clouds on a global basis. The two parameters needed to assess horizontal homogeneity are, thus, the regional area  $A$ , and the contrast threshold  $T$ . For this study,  $A$  is taken to be square, and an integral multiple of the 275 m level 1B2 grid resolution.  $T$  is defined as the maximum difference in reflectivities occurring across  $A$  expressed as a percentage of the reflectance at the central pixel of  $A$ .

[15] In order to derive a result somewhat independent of natural variations in global cloudiness, it was necessary to minimize the effect of such variations within our study by processing extremely large amount of satellite data. To facilitate this approach we developed a quasi-deterministic and computationally efficient method for classifying scene homogeneity. For a given threshold  $T$ , we start with the bidirectional reflectance  $r$  of the central pixel in  $A$ , where  $r = \pi * L / F_{\text{solar}}$  with  $L$  being the measured spectral radiance, and  $F_{\text{solar}}$  the spectral solar irradiance. The value of  $r$  for the central pixel is then compared with the reflectance of a different pixel in  $A$ . Should the difference between the two values of  $r$  exceed  $T/2$ , then the remaining pixels in  $A$  are skipped and the region is labeled as heterogeneous. Otherwise we continue to compare the value  $r$  for the central pixel with the values of  $r$  for other pixels within  $A$ . If the difference in  $r$  remains less than  $T/2$  for the remaining

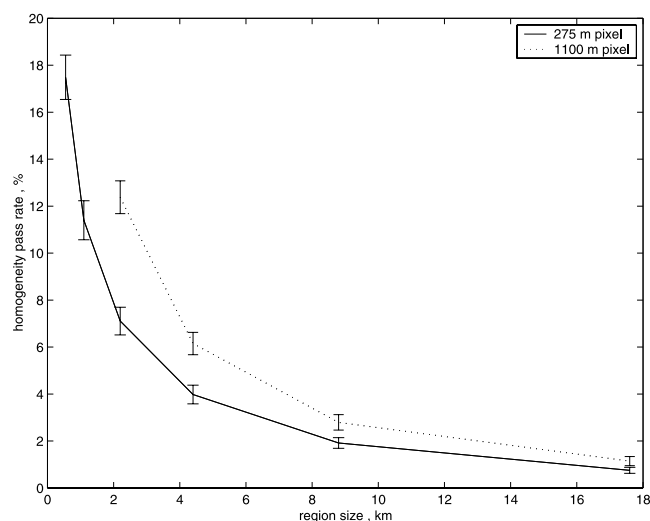


**Figure 2.** Dependence of the spatial homogeneity pass rate on region size and resolution for 14 orbits on 9 April 2001 (solid line—275 m pixel resolution, dotted line—1100 m pixel resolution).

pixels, then A is labeled as homogeneous. This computational compromise results in the following interpretation of the result. Horizontal homogeneity for a threshold  $T = 10\%$  implies that the maximum range of reflectances within A is less than 10%. Heterogeneity for  $T = 10\%$  implies that the minimum range of reflectances within A is greater than 5%. Note that if the range of reflectances in A lies between 5 and 10%, the area will be randomly labeled as homogeneous or heterogeneous depending on how close the value of  $r$  for the starting pixel is to the average reflectance for the region. Since our application is to an extremely large data set, the percentage of regions classified as homogeneous for a given value of  $T$  can be interpreted as the percentage of regions for which the range of reflectances is actually less than  $0.75T$ .

### 2.3. Analysis Approach

[16] The analysis of each case comprised setting the following variables (default values in parentheses): homogeneity threshold  $T$  (10%); pixel resolution (275 m); regional area A ( $[8.8 \text{ km}]^2$  or  $32 \times 32$  pixels); viewing direction (nadir); spectral band (672 nm); and latitude range ( $55^\circ\text{S}$  to  $65^\circ\text{N}$ ). In addition, dark scenes, especially thin cloud and most clear scenes over ocean, were also excluded by adopting a constant reflectance threshold of  $r = 0.2$ . The homogeneity pass rate was accumulated for each orbit, and these pass rates then averaged over all orbits. Since the orbital pass rates appeared to be reasonably independent of each other, we use their standard deviation to estimate the expected uncertainty in the overall mean due to natural variability.

## 3. Results

### 3.1. Overall Cloud Homogeneity

[17] Applying the analysis with the above default values (i.e., excluding dark scenes and high latitudes, with a tolerance of  $\pm 5\%$  in reflectance over an 8.8 km square) to the entire 58 orbits, we obtained a homogeneity pass rate of

$(1.4 \pm 0.3)\%$ , where the uncertainty is due to the effects of natural variability on our limited data set.

#### 3.1.1. High Latitude Effect

[18] Relaxing the high latitude constraint to include all data above the reflectance threshold increased the data volume by about 15% and raised the pass rate to  $(2.8 \pm 0.3)\%$ , suggesting that high latitude of snow and ice regions tend to be far more homogeneous than heterogeneous.

#### 3.1.2. Degraded Resolution

[19] When the original level 1B2 data are degraded to an 1100 m resolution by averaging  $4 \times 4$  pixels, characteristic of some MISR global mode data, and the analysis repeated, the homogeneity pass rate rises to  $(2.3 \pm 0.5)\%$ , about 1.6 times the full resolution value. The higher agreement between spatially averaged radiances would likely continue to increase if the spatial resolution were to be degraded further, which is of relevance to statistical correlation studies. We note here, however, that there a significant reduction in apparent homogeneity is evident when using the higher resolution of MISR compared to that of sensors such as ERBE, AVHRR, etc.

### 3.2. Effect of Region Size

[20] The effect of region size on the homogeneity pass rate was examined, choosing (square) dimensions of 550 m, 1100 m, 2200 m, 4400 m, 8800 m, and 17,600 m, at both normal (275 m) resolution and degraded (1100 m) resolution. Here the results of section 3.1 were used, for computational efficiency, to limit the data to 14 orbits from a single day, 9 April 2001, due to the fact that this day had a slightly higher pass rate than the average for the larger set of 58 orbits. Figure 2 shows an increase in the pass rate as the region is reduced in size. Error bars indicate the effect of natural variability on the pass rate. Note that even for a region size of 1.1 km, for which one might expect the subpixel variation to be relatively minor when considered globally, the homogeneity pass rate is still low, at about 11%. The pass rates are about 60% higher for degraded resolution than for normal resolution, irrespective of region size.

### 3.3. Effects of Threshold and View Angle

[21] Four orbits on 9 April 2001 (paths 026, 131, 211, and 227) were chosen for additional analysis, to examine the effects of homogeneity threshold and viewing angle on the pass rate. As might be expected, the pass rates rises steadily with increasing threshold. Figure 3 shows that this rise is relatively linear for each of the nine cameras, for thresholds greater than a few percent.

[22] For a given threshold, the pass rate is lowest for the nadir view (An camera) and rises systematically with increasing viewing angle. This result is qualitatively similar to that noted in the spatial autocorrelation of ERBE radiances, which also increases with view angle even when changes in resolution with view angle have been removed [Davies, 1994]. In the present case, the increased pass rate with view angle is likely due to the intrinsic reduction in spatial variability with angle shown by Davies [1994], as well as to the decreased resolution. The smaller differences that are evident for the same view-angle pairs (Da-Df and Ca-Cf) are more likely due to the effects of natural variability associated with the smaller amount of data used

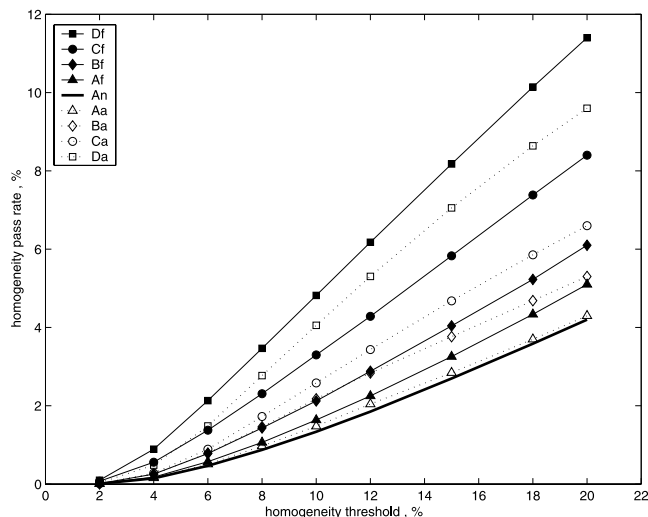


**Figure 3.** Dependence of the spatial homogeneity pass rate on the homogeneity threshold for each of the nine MISR cameras. Data from paths 26, 131, 211, and 227 on 9 April 2001.

in this analysis, than to other factors, given the statistical symmetry of the scattering angles of the fore and aft members of the camera pair.

#### 4. Summary

[23] Very few mid-morning clouds passed our test for spatially homogeneous reflectivity. Only about 1 in 70 ( $1.4 \pm 0.3\%$ ) of globally distributed 8.8 km square cloudy regions had uniform reflectivity within  $\pm 5\%$  of their central values when these values exceeded 0.2, and when measurements were made at a nominal resolution of 275 m. Although this result is strictly applicable to mid-morning clouds only, it may be indicative of clouds more generally, given the weak diurnal variation of ocean clouds, and competing heterogeneous (cumuliform) and homogeneous (anvil cirrus) diurnal influences over land.

[24] As the region considered is reduced in size, its reflectivity appears more uniform, so that about 1 in 14 (7%) of 2.2 km regions, and 1 in 9 (11%) of 1.1 km regions now pass the same test. Similarly, if the homogeneity criterion is relaxed by a factor of two, so the reflectivities across the region can vary by  $\pm 10\%$  from the central value

(i.e., ranging through an average of 15%), then the pass rate rises by a factor of almost 3.

[25] We conclude that there is a globally significant subset of all clouds, between about 1 in 10 and about 1 in 100 depending on the resolution, that appear to be spatially uniform, and for which one-dimensional retrieval techniques of cloud optical properties can be applied with confidence. The remaining clouds appear to be spatially heterogeneous at high resolution, which may call into question the applicability of conventional one-dimensional inversion techniques that are resolution dependent.

[26] **Acknowledgments.** Much of this research was supported by the Jet Propulsion Laboratory of the California Institute of Technology under Contract 960489 to the University of Arizona. IG acknowledges an NSF-NATO Fellowship for Engineering and Science. We thank P. Zuidema, T. Várnai, A. Horváth, M. J. Garay, R. Kahn and D. J. Diner for helpful discussions, and C. Moroney for assistance with the data acquisition.

#### References

- Bruegge, C. J., N. L. Chrien, R. R. Ando, D. J. Diner, W. A. Abdou, M. C. Helmlinger, S. H. Pilon, and K. J. Thome, Early validation of the Multi-angle Imaging SpectroRadiometer (MISR) radiometric scale, *IEEE Trans. Geosci. Remote Sensing*, *40*, 1477–1492, 2002.
- Davies, R., Spatial autocorrelation of radiation measured by the Earth Radiation Budget Experiment: Scene inhomogeneity and reciprocity violation, *J. Geophys. Res.*, *99*, 20,879–20,887, 1994.
- Di Girolamo, L., and R. Davies, Cloud fraction errors caused by finite resolution measurements, *J. Geophys. Res.*, *102*, 1739–1756, 1997.
- Diner, D. J., et al., Multi-angle Imaging SpectroRadiometer (MISR) instrument description and experiment overview, *IEEE Trans. Geosci. Remote Sensing*, *36*, 1072–1087, 1998.
- Loeb, N. G., and J. A. Coakley Jr., Inference of marine stratus cloud optical depths from satellite measurements: Does 1D theory apply?, *J. Clim.*, *11*, 215–233, 1998.
- Loeb, N. G., and R. Davies, Observational evidence of plane parallel model biases: The apparent dependence of cloud optical depth on solar zenith angle, *J. Geophys. Res.*, *101*, 1621–1634, 1996.
- Loeb, N. G., T. Várnai, and R. Davies, Effect of cloud inhomogeneities on the solar zenith angle dependence of nadir reflectance, *J. Geophys. Res.*, *102*, 9387–9395, 1997.
- Oreopoulos, L., and R. Davies, Plane parallel albedo biases from satellite observations. Part I: Dependence on resolution and other factors, *J. Clim.*, *11*, 919–932, 1998.
- Rossow, W. B., C. Delo, and B. Cairns, Implications of the observed mesoscale variations of clouds for the Earth's radiation budget, *J. Clim.*, *15*, 557–585, 2002.
- Wielicki, B. A., and L. Parker, On the determination of cloud cover from satellite sensors—the effect of sensor resolution, *J. Geophys. Res.*, *97*, 12,799–12,823, 1992.

R. Davies, Jet Propulsion Laboratory/California Institute of Technology, Pasadena, CA, USA.

I. Genkova, Pacific Northwest National Laboratory, Richland, WA, USA. (iliana.genkova@pnl.gov)